







OPEN

Stable isotope variations of dew under three different climates

DATA DESCRIPTOR

Chao Tian^{1,2,3}, Kun Du^{1,3,4,5}, Lixin Wang²  , Xiao Zhang⁶, Fadong Li^{1,3,5}, Wenzhe Jiao², Daniel Beysens^{7,8} , Kudzai Farai Kaseke^{2,9}  & Marie-Gabrielle Medici¹⁰

As a supplementary or the only water source in dry regions, dew plays a critical role in the survival of organisms. The new hydrological tracer ¹⁷O-excess, with almost sole dependence on relative humidity, provides a new way to distinguish the evaporation processes and reconstruct the paleoclimate. Up to now, there is no published daily dew isotope record on $\delta^2\text{H}$, $\delta^{18}\text{O}$, $\delta^{17}\text{O}$, d-excess, and ¹⁷O-excess. Here, we collected daily dew between July 2014 and April 2018 from three distinct climatic regions (i.e., Gobabeb in the central Namib Desert with desert climate, Nice in France with Mediterranean climate, and Indianapolis in the central United States with humid continental climate). The $\delta^2\text{H}$, $\delta^{18}\text{O}$, and $\delta^{17}\text{O}$ of dew were simultaneously analyzed using a Triple Water Vapor Isotope Analyzer based on Off-Axis Integrated Cavity Output Spectroscopy technique, and then d-excess and ¹⁷O-excess were calculated. This report presents daily dew isotope dataset under three climatic regions. It is useful for researchers to use it as a reference when studying global dew dynamics and dew formation mechanisms.

Background & Summary

Global warming has increased the demand of moisture in the local atmosphere, leading to a decrease in precipitation over many regions, both of which could contribute to drought^{1,2}. Water vapor can condense as dew on a surface where radiation cools below the dew point temperature^{3,4}. Dew, as a significant source of non-rainfall water, is considered a vital water source due to its considerable contribution for the surface water balance, especially in semiarid and arid regions^{3,5–8}. The annual dew amounts account for 9% to 23% of rainfall in arid regions^{7,9}. Dew could be used as an alternative source of water during dry season of tropical islands¹⁰. Dew is beneficial to the survival, growth and development of the plants in arid regions or during droughts, such as bringing nocturnal moisture^{11–13} and being directly absorbed and utilized by leaves through plant stomata or special physical features (e.g., aerial plants)^{14–16}. Thus, dew could increase net photosynthate accumulation in leaves¹⁷ and improve plant water use efficiency^{16,18}. Dew is also involved in the chemical processes in the atmosphere, such as the diurnal (and nocturnal) cycle of nitrites oxides^{3,19}. Dew frequency decreased by 5.2 days per decade from 1961 to 2010 in China due primarily to near-surface warming and associated decreases in relative humidity (RH)¹¹. Furthermore, the decreasing rate of dew frequency in arid regions (50%) is higher than that in semi-humid and humid regions in China (40% and 28%)¹¹. Therefore, dew in different regions have different trends with the global climate change, and dew characteristics under different climate regions are needed to better predict future changes in dew dynamics.

$\delta^2\text{H}$ and $\delta^{18}\text{O}$ are natural and traditional hydrological tracers, and play an important role to trace different hydrometeorological processes associated with different types of waters (e.g., rainfall, snowfall, dew, fog, surface water, plant water, and ice core)^{20–24}. Two types of mass-dependent fractionation process, equilibrium

¹Key Laboratory of Ecosystem Network Observation and Modeling, Institute of Geographic Sciences and Natural Resources Research, Chinese Academy of Sciences, Beijing, 100101, China. ²Department of Earth Sciences, Indiana University-Purdue University Indianapolis (IUPUI), Indianapolis, IN, 46202, USA. ³Shandong Yucheng Agroecosystem National Observation and Research Station, Ministry of Science and Technology, Yucheng, 251200, China. ⁴School of Resources and Environment, LinYi University, Linyi, 276000, China. ⁵College of Resources and Environment, University of Chinese Academy of Sciences, Beijing, 100049, China. ⁶Key Laboratory of Geospatial Technology for the Middle and Lower Yellow River Regions, Ministry of Education. College of Environment and Planning, Henan University, Jinming Avenue, Kaifeng, 475004, China. ⁷Physique et Mécanique des Milieux Hétérogènes, CNRS, ESPCI, PSL Research University, Sorbonne Université, Sorbonne Paris Cité, 75005, Paris, France. ⁸OPUR, 2 rue Verderet, 75016, Paris, France. ⁹Earth Research Institute, University of California, Santa Barbara, CA, 93106, USA. ¹⁰LPMC, Université de Nice, CNRS-UMR 7336, 06108, Nice Cedex 2, France. ✉e-mail: lxwang@iupui.edu

| Site (Country) | Latitude (°) | Longitude (°) | Elevation (m, a.s.l.) | Köppen climate classification | $\delta^2\text{H}$ (‰) | $\delta^{18}\text{O}$ (‰) | $\delta^{17}\text{O}$ (‰) | d-excess (‰) | ^{17}O -excess (per meg) | Temperature (°C) | Relative Humidity (%) | Vapor Pressure Deficit (hPa) | |
|-----------------------------|--------------|---------------|-----------------------|-------------------------------|------------------------|---------------------------|---------------------------|--------------|-----------------------------------|------------------|-----------------------|------------------------------|------|
| Gobabeb (Namibia) | −23.55 | 15.04 | 405 | Desert climate | Minimum | −33.21 | −6.77 | −3.55 | −19.9 | −39 | 3.53 | 35.3 | 1.3 |
| | | | | | Maximum | 18.17 | 3.23 | 1.66 | 26.5 | 45 | 16.85 | 98.3 | 52.7 |
| | | | | | Mean | −5.11 | −1.43 | −0.75 | 6.3 | 9 | 11.83 | 77.6 | 17.1 |
| | | | | | Standard deviation | 14.03 | 2.59 | 1.35 | 10.0 | 22 | 3.67 | 17.8 | 14.2 |
| Nice (France) | 43.74 | 7.27 | 310 | Mediterranean climate | Minimum | −114.77 | −16.65 | −8.79 | 0.1 | 7 | 3.55 | 55.1 | 4.6 |
| | | | | | Maximum | −1.90 | −0.70 | −0.36 | 32.3 | 54 | 15.25 | 94.2 | 31.0 |
| | | | | | Mean | −37.92 | −7.00 | −3.67 | 18.1 | 34 | 9.06 | 80.4 | 14.0 |
| | | | | | Standard deviation | 25.91 | 3.75 | 1.99 | 8.8 | 12 | 3.01 | 9.6 | 6.6 |
| Indianapolis (United State) | 39.88 | −86.27 | 258 | Humid continental climate | Minimum | −83.99 | −13.39 | −7.06 | −5.0 | −5 | 1.39 | 65.9 | 0.2 |
| | | | | | Maximum | −1.34 | 0.46 | 0.24 | 32.1 | 64 | 21.36 | 99.8 | 27.1 |
| | | | | | Mean | −39.38 | −6.51 | −3.41 | 12.7 | 35 | 13.91 | 91.9 | 6.2 |
| | | | | | Standard deviation | 19.81 | 3.10 | 1.64 | 7.2 | 11 | 4.39 | 6.5 | 5.0 |

Table 1. Summary of the daily dew record at Gobabeb (from July 2014 to June 2017), Nice (from December 2017 to April 2018), and Indianapolis (from January 2017 to October 2017).

fractionation and kinetic fractionation, is the fundamental cause of isotope differences during water phase change^{25–28}. They are mainly determined by the saturation vapor pressure and the diffusion rate of different isotopes, respectively^{29–31}.

^{17}O -excess (^{17}O -excess = $\ln(\delta^{17}\text{O} + 1) - 0.528 \times \ln(\delta^{18}\text{O} + 1)$), a newer hydrological tracer, became available to provide additional constraints about moisture transport, rainout, and evaporation to probe hydrological and meteorological processes^{32,33}. Compared with the conventional isotopes depending on both temperature and RH, the ^{17}O -excess is mainly sensitive to the RH between 10°C to 45°C^{34,35}. The RH dependence is also confirmed by field experimental observations such as monsoon precipitation and leaf water in Africa^{36,37}, precipitation on a subtropical island³⁸, surface water across the Pacific Northwest, USA³⁹, and ice cores in coastal East Antarctica⁴⁰. The relationship between $\delta^{18}\text{O}$ and $\delta^{17}\text{O}$ (i.e., the slope of $1000 \times \ln(\delta^{18}\text{O} + 1)$ and $1000 \times \ln(\delta^{17}\text{O} + 1)$)⁴¹ can be used to better reveal tap water and precipitation formation mechanisms⁴², differentiate drought types (e.g., synoptic drought vs. local drought)⁴³, and distinguish different types of condensation (e.g., fog vs. dew) in the Namib Desert⁴⁴. Furthermore, it is an effective method to infer the different water evaporation processes experiencing equilibrium fractionation or kinetic fractionation using the relationships between ^{17}O -excess and $\delta^{18}\text{O}$ (or d-excess) (e.g., laboratory model test, precipitation, and natural water bodies (river, channels, wells, springs, groundwater, lake and ponds))^{32,34,36,45–50}.

To the best of our knowledge, there is no daily dew isotope dataset including ^{17}O -excess publicly available. Here, we provide daily dew isotope dataset ($\delta^2\text{H}$, $\delta^{18}\text{O}$, $\delta^{17}\text{O}$, d-excess, and ^{17}O -excess) under three different climatic regions including Gobabeb–Namib Research Institute (hereafter Gobabeb) in the central Namib Desert with desert climate, Nice in France with Mediterranean climate, and Indianapolis in the central United States with humid continental climate collected between July 2014 to April 2018. Our previous studies have described the operating procedures of Triple Water Vapor Isotope Analyzer (T-WVIA-45-EP; Los Gatos Research Inc. (LGR), Mountain View, CA, USA) based on Off-Axis Integrated Cavity Output Spectroscopy (OA-ICOS) technique^{46,51}, as well as the detailed description of ^{17}O -excess quality control method. The dew isotopic variations have been published in Tian *et al.*⁵². This first publicly available daily dew isotope dataset were presented to fill the gap in global non-rainfall water isotope datasets, especially for ^{17}O -excess. This would provide data support for scientists to study the global dew distribution characteristics and formation mechanism under climate change.

Methods

Sample collections. The daily dew samples were collected in three different climatic regions including 22 samples in Gobabeb (23.55° S, 15.04° E; 405 m above sea level) with desert climate from July 2014 to June 2017, 23 samples in Nice (43.74° N, 7.27° E; 310 m above sea level) with Mediterranean climate from December 2017 to April 2018, and 69 samples in Indianapolis (39.88° N, 86.27° W; 258 m above sea level) with humid continental climate from January 2017 to October 2017. The detail site meteorological information has been described by Tian *et al.*⁵². In short, the mean annual temperature (hereafter MAT), mean annual relative humidity (hereafter MARH), and mean annual precipitation amount (hereafter MAP) in Gobabeb is 21.1°C, 50%, and < 20 mm, respectively. The MAT, MARH, and MAP in Nice is 16.0°C, 78%, and 733 mm, respectively. The MAT, MARH, and MAP in Indianapolis is 10.2°C, 69%, and 953 mm, respectively. For Gobabeb, there are concurrent fog and dew collectors installed at the same location, collected water samples were considered dew when water samples appear in dew collector and no samples in the fog collector. For Nice and Indianapolis, fog is rarely seen, dew samples were separated from fog or light rain based on local meteorological information and visual observation of the collecting personnel. All of daily dew samples were collected before dawn to minimize evaporation effects

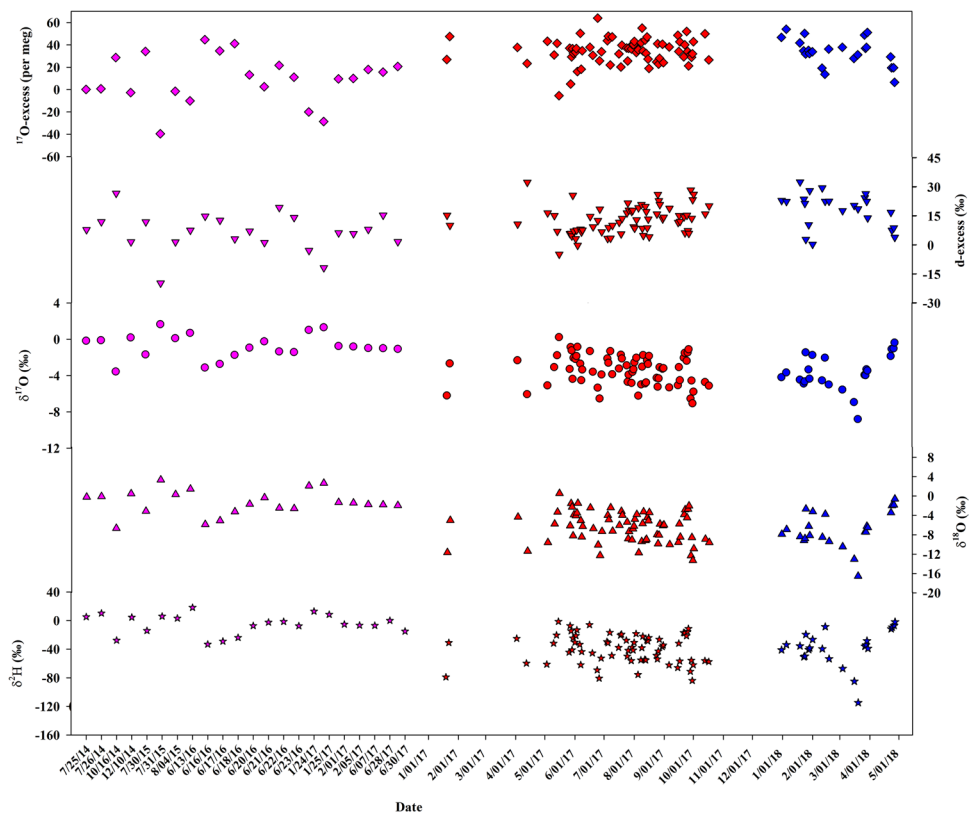


Fig. 1 Dew stable isotope variations at Gobabeb (purple colors), Nice (blue colors), and Indianapolis (red colors). From top to bottom: ^{17}O -excess, d-excess, $\delta^{17}\text{O}$, $\delta^{18}\text{O}$, and $\delta^2\text{H}$ modified from Tian *et al.*⁵².

on isotopes, and they were stored in 15 ml sealed glass vials in Gobabeb and Indianapolis or polyethylene bottles for the dew samples in Nice. All of the 114 dew samples were delivered to the IUPUI (Indiana University-Purdue University Indianapolis) Ecohydrology Lab to measure $\delta^2\text{H}$, $\delta^{18}\text{O}$ and $\delta^{17}\text{O}$. Here, the detailed daily dew isotopic variations were reported especially for ^{17}O -excess values.

Isotope measurements and ^{17}O -excess data processing. The isotopic variations was measured using a Triple Water Vapor Isotope Analyzer (T-WVIA-45-EP, Los Gatos Research Inc. (LGR), Mountain View, CA, USA; preheated to 50°C) coupled to a Water Vapor Isotope Standard Source (WVISS, LGR, Mountain View, CA, USA; preheated to 80°C)⁵³. The detailed operation has been described by Tian *et al.*^{42,51}. To ensure the accuracy of the T-WVIA performance, LGR#1 to LGR#5 as five working standards from LGR were analyzed after every five samples. The known $\delta^2\text{H}$ from LGR#1 to LGR#5 is -154.0‰ , -123.7‰ , -97.3‰ , -51.6‰ , and -9.2‰ , respectively. The known $\delta^{18}\text{O}$ from LGR#1 to LGR#5 is -19.49‰ , -16.24‰ , -13.39‰ , -7.94‰ , and -2.69‰ , respectively. The known $\delta^{17}\text{O}$ from LGR#1 to LGR#5 is -10.30‰ , -8.56‰ , -7.06‰ , -4.17‰ , and -1.39‰ , respectively. Additionally, to reduce differences between laboratories, all of the isotope ratios were normalized using Vienna Standard Mean Ocean Water (VSMOW) and Standard Light Antarctic Precipitation (SLAP) once a day^{54,55}. The $\delta^2\text{H}$, $\delta^{18}\text{O}$, and $\delta^{17}\text{O}$ of SLAP are -427.5‰ , -55.5‰ , and -29.6986‰ , respectively^{55,56}. Furthermore, ^{17}O -excess with small order of magnitude, need to quality control using raw $\delta^{17}\text{O}$ and $\delta^{18}\text{O}$ values to obtain accurate value. The detailed quality-control steps could be found in our previous studies^{46,51}. To summarize, each individual data point was checked using two types of quality control filters. Firstly, because regression coefficient λ ($\lambda = \ln(\delta^{17}\text{O} + 1)/\ln(\delta^{18}\text{O} + 1)$) is the same as mass-dependent fractionation coefficient (θ) during liquid-vapor equilibrium and in water vapor diffusion in air^{34,57}, and theoretically the θ was found to be 0.511 ± 0.005 for kinetic transport effects⁵⁷ and 0.529 ± 0.001 for equilibrium effects³⁴. Individual data points with regression coefficient λ outside the range of 0.506 and 0.530 were removed. Secondly, ^{17}O -excess values that exceed the range of -100 to $+100$ per meg were removed, which exceed the range of observed global precipitation ^{17}O -excess values^{34,36,47,57,58}. The final ^{17}O -excess value of each dew sample was the mean value of all the individual data points meet the above the two conditions.

Data Records

Daily dew isotope database is archived in PANGAEA in a single table including 114 rows and 13 columns⁵⁹. Each row presents a daily dew event at one site. Each column corresponds to the geographic location information (including latitude, longitude, and elevation), isotope variables including three measured individual stable isotopes ($\delta^2\text{H}$, $\delta^{18}\text{O}$, and $\delta^{17}\text{O}$) and two calculated second-order isotopic variables (d-excess and ^{17}O -excess), and three meteorological information including temperature, RH, and VPD. A summary of the dew from July 2014

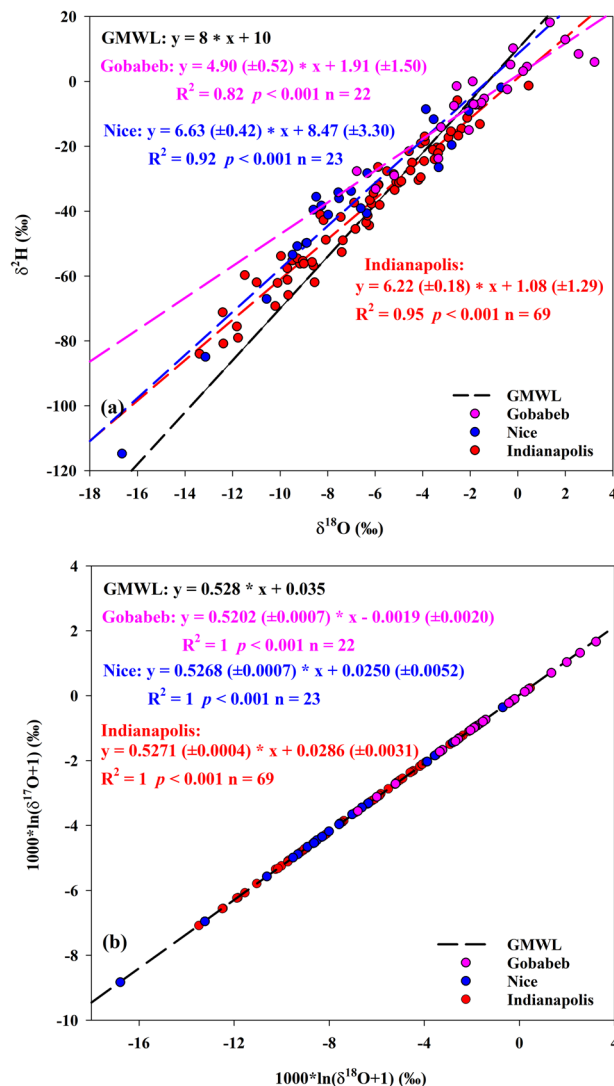


Fig. 2 The relationships between $\delta^{18}\text{O}$ and $\delta^{2}\text{H}$ (a), as well as between $\delta^{18}\text{O}$ and $\delta^{17}\text{O}$ based on daily dew at Gobabeb, Nice, and Indianapolis.

to April 2018 under three different climatic regions (Gobabeb, Nice, and Indianapolis) is presented in Table 1. The database spanned a large gap over 67.29° in latitude (from 23.55°S to 43.74°N) and 101.3° in longitude (from 86.27°W to 15.04°E). However, the difference in elevation was relatively small ranging from 258 m to 405 m. The meteorological factors show significant difference ranging from 1.39°C to 21.36°C for temperature, from 35.3% to 99.8% for RH, and from 0.2 hPa to 52.7 hPa for VPD (Table 1). Figure 1 depicts the distribution of daily dew stable isotopes in the three sites, which was modified from our previous study⁵². As for the dew in Gobabeb, the $\delta^{2}\text{H}$ values varied from -33.21‰ to 18.17‰ with a mean value of $-5.11 \pm 14.03\text{‰}$. The $\delta^{18}\text{O}$ values varied from -6.77‰ to 3.23‰ with a mean value of $-1.43 \pm 2.59\text{‰}$. The $\delta^{17}\text{O}$ values varied from -3.55‰ to 1.66‰ with a mean value of $-0.75 \pm 1.35\text{‰}$. The d-excess values varied from -19.9‰ to 26.5‰ with a mean value of $6.3 \pm 10.0\text{‰}$. The ^{17}O -excess values varied from -39 to 45 per meg with a mean value of 9 ± 22 per meg. As for the dew in Nice, the $\delta^{2}\text{H}$ values varied from -114.77‰ to -1.90‰ with a mean value of $-37.92 \pm 25.91\text{‰}$. The $\delta^{18}\text{O}$ values varied from -16.65‰ to -0.70‰ with a mean value of $-7.00 \pm 3.75\text{‰}$. The $\delta^{17}\text{O}$ values varied from -8.79‰ to -0.36‰ with a mean value of $-3.67 \pm 1.99\text{‰}$. The d-excess values varied from 0.1‰ to 32.3‰ with a mean value of $18.1 \pm 8.8\text{‰}$. The ^{17}O -excess values varied from 7 to 54 per meg with a mean value of 34 ± 12 per meg. As for the dew in Indianapolis, the $\delta^{2}\text{H}$ values varied from -83.99‰ to -1.34‰ with a mean value of $-39.38 \pm 19.81\text{‰}$. The $\delta^{18}\text{O}$ values varied from -13.39‰ to 0.46‰ with a mean value of $-6.51 \pm 3.10\text{‰}$. The $\delta^{17}\text{O}$ values varied from -7.06‰ to 0.24‰ with a mean value of $-3.41 \pm 1.64\text{‰}$. The d-excess values varied from -5.0‰ to 32.1‰ with a mean value of $12.7 \pm 7.2\text{‰}$. The ^{17}O -excess values varied from -5 to 64 per meg with a mean value of 35 ± 11 per meg. Linear least-squares fitting was utilized to determine the slope and intercept of the dew line in the three sites. The numbers in the parenthesis were standard errors of the estimates. The dew line in Gobabeb between $\delta^{18}\text{O}$ and $\delta^{2}\text{H}$ was $\delta^{2}\text{H} = 4.90 (\pm 0.52) * \delta^{18}\text{O} + 1.91 (\pm 1.50)$ ($R^2 = 0.82$, $p < 0.001$), which had the lowest slope and intercept than those in Nice and Indianapolis (Fig. 2a). The slope and

intercept in Nice were 6.63 and 8.47, and those in Indianapolis were 6.22 and 1.08. All of the three dew lines were far from the Global Meteoric Water Line (GMWL, $\delta^2\text{H} = 8 \times \delta^{18}\text{O} + 10$). The dew line in Gobabeb between $\delta^{18}\text{O}$ and $\delta^{17}\text{O}$ was $\delta^{17}\text{O} = 0.5202 (\pm 0.0007) \times \delta^{18}\text{O} - 0.0019 (\pm 0.0020)$ ($R^2 = 1$, $p < 0.001$), far from the GMWL for oxygen ($\delta^{17}\text{O} = 0.528 \times \delta^{18}\text{O} + 0.035$, normalized to the VSMOW-SLAP scale^{47,58} (Fig. 2b). The slope and intercept of the dew line between $\delta^{18}\text{O}$ and $\delta^{17}\text{O}$ in Nice (0.5268 and 0.0250) was similar with those in Indianapolis (0.5271 and 0.0286), both of which were close to the GMWL.

Technical Validation

The precisions of different isotopic variables for two international standards (SLAP and Greenland Ice Sheet Precipitation) and the five working standards (LGR#1 to LGR#5) have been measured in our previous studies, which was $<0.80\text{‰}$, $<0.06\text{‰}$, $<0.03\text{‰}$, and <12 per meg for $\delta^2\text{H}$, $\delta^{18}\text{O}$, $\delta^{17}\text{O}$, and ^{17}O -excess, respectively^{42,51}. The precisions of our OA-ICOS measurements are within the range of analyzers using the same technique (0.07‰, 0.05‰, and 10 to 18 per meg for $\delta^{18}\text{O}$, $\delta^{17}\text{O}$, and ^{17}O -excess, respectively)⁶⁰. Comparing with the Cavity Ring Down Spectroscopy (CRDS) technique, our precisions are comparable with previous studies ($<0.98\text{‰}$, $<0.10\text{‰}$, $<0.10\text{‰}$, and <10 per meg for $\delta^2\text{H}$, $\delta^{18}\text{O}$, $\delta^{17}\text{O}$, and ^{17}O -excess, respectively)^{54,61}. Our precisions are also acceptable compared with the traditional Isotope Ratio Mass Spectrometry (IRMS) technique ($<0.7\text{‰}$, $<0.3\text{‰}$, $<0.05\text{‰}$, and <16 per meg for $\delta^2\text{H}$, $\delta^{18}\text{O}$, $\delta^{17}\text{O}$, and ^{17}O -excess, respectively)^{47,55,58,62}.

Code availability

No custom code was used to generate or process the data.

Received: 25 August 2021; Accepted: 11 January 2022;

Published online: 14 February 2022

References

- Dai, A., Zhao, T. & Chen, J. Climate Change and Drought: a Precipitation and Evaporation Perspective. *Curr. Clim. Change Rep.* **4**, 301–312 (2018).
- Jiao, W., Wang, L. & McCabe, M. F. Multi-sensor remote sensing for drought characterization: current status, opportunities and a roadmap for the future. *Remote Sens. Environ.* **256**, 112313 (2021).
- Beysens, D. *Dew Water*. (River Publishers, 2018).
- Monteith, J. & Unsworth, M. *Principles of environmental physics: plants, animals, and the atmosphere*. (Academic Press, 2013).
- Wang, L., Kaseke, K. F. & Seely, M. K. Effects of non-rainfall water inputs on ecosystem functions. *WIRES. Water* **4**, e1179 (2017).
- Jacobs, A. F. G., Heusinkveld, B. G. & Berkowicz, S. M. Dew deposition and drying in a desert system: a simple simulation model. *J. Arid Environ.* **42**, 211–222 (1999).
- Ucles, O., Villagarcia, L., Moro, M. J., Canton, Y. & Domingo, F. Role of dewfall in the water balance of a semiarid coastal steppe ecosystem. *Hydrol. Process.* **28**, 2271–2280 (2014).
- Charnes, A., Cooper, W. W. & Rhodes, E. Measuring the efficiency of decision making units. *European journal of operational research* **2**, 429–444 (1978).
- Malek, E., McCurdy, G. & Giles, B. Dew contribution to the annual water balances in semi-arid desert valleys. *J. Arid Environ.* **42**, 71–80 (1999).
- Muselli, M., Clus, O., Ortega, P., Milimouk, I. & Beysens, D. Physical, Chemical and Biological Characteristics of Dew and Rainwater during the Dry Season of Tropical Islands. *Atmosphere* **12**, 69 (2021).
- Dou, Y., Quan, J., Jia, X., Wang, Q. & Liu, Y. Near-Surface Warming Reduces Dew Frequency in China. *Geophys. Res. Lett.* **48**, e2020GL091923 (2021).
- Trosseille, J., Mongruel, A., Royon, L. & Beysens, D. Radiative cooling for dew condensation. *Int. J. Heat Mass Tran.* **172**, 121160 (2021).
- Steinberger, Y., Loboda, I. & Garner, W. The Influence of Autumn Dewfall on Spatial and Temporal Distribution of Nematodes in the Desert Ecosystem. *J. Arid Environ.* **16**, 177–183 (1989).
- Gerlein-Safdi, C. *et al.* Dew deposition suppresses transpiration and carbon uptake in leaves. *Agr. Forest Meteorol.* **259**, 305–316 (2018).
- Berry, Z. C., Emery, N. C., Gotsch, S. G. & Goldsmith, G. R. Foliar water uptake: Processes, pathways, and integration into plant water budgets. *Plant Cell Environ.* **42**, 410–423 (2019).
- Monteith, J. L. & Unsworth, M. H. *Principles of environmental physics Second edition*. (Edward Arnold, 1990).
- Zhuang, Y. & Ratcliffe, S. Relationship between dew presence and *Bassia dasyphylla* plant growth. *J. Arid Land* **4**, 11–18 (2012).
- Ben-Asher, J., Alpert, P. & Ben-Zvi, A. Dew is a major factor affecting vegetation water use efficiency rather than a source of water in the eastern Mediterranean area. *Water Resour. Res.* **46**, W10532 (2010).
- Tomaszkiewicz, M., Abou Najm, M., Beysens, D., Alameddine, I. & El-Fadel, M. Dew as a sustainable non-conventional water resource: a critical review. *Environ. Rev.* **23**, 425–442 (2015).
- Dansgaard, W. Stable isotopes in precipitation. *Tellus* **16**, 436–468 (1964).
- Jouzel, J. & Merlivat, L. Deuterium and oxygen 18 in precipitation: Modeling of the isotopic effects during snow formation. *J. Geophys. Res.* **89**, 11749–11757 (1984).
- Wang, L. *et al.* Partitioning evapotranspiration across gradients of woody plant cover: Assessment of a stable isotope technique. *Geophys. Res. Lett.* **37**, L09401 (2010).
- Lanning, M., Wang, L., Benson, M., Zhang, Q. & Novick, K. A. Canopy isotopic investigation reveals different water uptake dynamics of maples and oaks. *Phytochemistry* **175**, 112389 (2020).
- Putman, A. L. & Bowen, G. J. A global database of the stable isotopic ratios of meteoric and terrestrial waters. *Hydrol. Earth Syst. Sc.* **23**, 4389–4396 (2019).
- Zhao, L. *et al.* Factors controlling spatial and seasonal distributions of precipitation $\delta^{18}\text{O}$ in China. *Hydrol. Process.* **26**, 143–152 (2012).
- Cui, J. *et al.* Quantifying the controls on evapotranspiration partitioning in the highest alpine meadow ecosystems. *Water Resour. Res.* **56** (2020).
- Soderberg, K., Good, S. P., Wang, L. & Caylor, K. Stable isotopes of water vapor in the vadose zone: A review of measurement and modeling techniques. *Vadose Zone J.* **11** (2012).
- Crawford, J., Hughes, C. E. & Parkes, S. D. Is the isotopic composition of event based precipitation driven by moisture source or synoptic scale weather in the Sydney Basin, Australia? *J. Hydrol.* **507**, 213–226 (2013).
- Griffis, T. J. Tracing the flow of carbon dioxide and water vapor between the biosphere and atmosphere: A review of optical isotope techniques and their application. *Agr. Forest Meteorol.* **174**, 85–109 (2013).

30. Winkler, R. *et al.* Interannual variation of water isotopologues at Vostok indicates a contribution from stratospheric water vapor. *Proc. Natl. Acad. Sci.* **110**, 17674–17679 (2013).
31. Jouzel, J. *et al.* Water isotopes as tools to document oceanic sources of precipitation. *Water Resour. Res.* **49**, 7469–7486 (2013).
32. Barkan, E. & Luz, B. Diffusivity fractionations of $\text{H}_2^{16}\text{O}/\text{H}_2^{17}\text{O}$ and $\text{H}_2^{16}\text{O}/\text{H}_2^{18}\text{O}$ in air and their implications for isotope hydrology. *Rapid Commun. Mass Spectrom.* **21**, 2999–3005 (2007).
33. Aron, P. G. *et al.* Triple oxygen isotopes in the water cycle. *Chem. Geol.* **565**, 120026 (2021).
34. Barkan, E. & Luz, B. High precision measurements of $^{17}\text{O}/^{16}\text{O}$ and $^{18}\text{O}/^{16}\text{O}$ ratios in H_2O . *Rapid Commun. Mass Spectrom.* **19**, 3737–3742 (2005).
35. Cao, X. & Liu, Y. Equilibrium mass-dependent fractionation relationships for triple oxygen isotopes. *Geochim. Cosmochim. Acta* **75**, 7435–7445 (2011).
36. Landais, A. *et al.* Combined measurements of ^{17}O -excess and d-excess in African monsoon precipitation: Implications for evaluating convective parameterizations. *Earth Planet. Sci. Lett.* **298**, 104–112 (2010).
37. Li, S., Levin, N. E., Soderberg, K., Dennis, K. J. & Caylor, K. K. Triple oxygen isotope composition of leaf waters in Mpala, central Kenya. *Earth Planet. Sci. Lett.* **468**, 38–50 (2017).
38. Uechi, Y. & Uemura, R. Dominant influence of the humidity in the moisture source region on the ^{17}O -excess in precipitation on a subtropical island. *Earth Planet. Sci. Lett.* **513**, 20–28 (2019).
39. Bershaw, J., Hansen, D. D. & Schauer, A. J. Deuterium excess and ^{17}O -excess variability in meteoric water across the Pacific Northwest, USA. *Tellus B.* **72**, 1773722 (2020).
40. Winkler, R. *et al.* Deglaciation records of ^{17}O -excess in East Antarctica: reliable reconstruction of oceanic normalized relative humidity from coastal sites. *Clim. Past* **8**, 1–16 (2012).
41. Meijer, H. & Li, W. The use of electrolysis for accurate $\delta^{17}\text{O}$ and $\delta^{18}\text{O}$ isotope measurements in water. *Isotopes Environ. Health Studies* **34**, 349–369 (1998).
42. Tian, C., Wang, L., Tian, F., Zhao, S. & Jiao, W. Spatial and temporal variations of tap water ^{17}O -excess in China. *Geochim. Cosmochim. Acta* **260**, 1–14 (2019).
43. Kaseke, K. F. *et al.* Precipitation origins and key drivers of precipitation isotope (^{18}O , ^2H , and ^{17}O) compositions over Windhoek, J. *Geophys. Res.* **123**, 7311–7330 (2018).
44. Kaseke, K. F., Wang, L. & Seely, M. K. Nonrainfall water origins and formation mechanisms. *Sci. adv.* **3**, e1603131 (2017).
45. Criss, R. E. *Principles of stable isotope distribution.* (Oxford University Press on Demand, 1999).
46. Tian, C., Wang, L., Kaseke, K. F. & Bird, B. W. Stable isotope compositions ($\delta^2\text{H}$, $\delta^{18}\text{O}$ and $\delta^{17}\text{O}$) of rainfall and snowfall in the central United States. *Sci. Rep.* **8**, 6712 (2018).
47. Li, S., Levin, N. E. & Chesson, L. A. Continental scale variation in ^{17}O -excess of meteoric waters in the United States. *Geochim. Cosmochim. Acta* **164**, 110–126 (2015).
48. Surma, J., Assonov, S., Bolourchi, M. & Staubwasser, M. Triple oxygen isotope signatures in evaporated water bodies from the Sistan Oasis, Iran. *Geophys. Res. Lett.* **42**, 8456–8462 (2015).
49. Surma, J., Assonov, S., Herwartz, D., Voigt, C. & Staubwasser, M. The evolution of ^{17}O -excess in surface water of the arid environment during recharge and evaporation. *Sci. Rep.* **8**, 4972 (2018).
50. Passey, B. H. & Ji, H. Triple oxygen isotope signatures of evaporation in lake waters and carbonates: A case study from the western United States. *Earth Planet. Sci. Lett.* **518**, 1–12 (2019).
51. Tian, C. & Wang, L. Stable isotope variations of daily precipitation from 2014–2018 in the central United States. *Sci. Data* **6**, 190018 (2019).
52. Tian, C. *et al.* Investigating the role of evaporation in dew formation under different climates using ^{17}O -excess. *J. Hydrol.* **592**, 125847 (2021).
53. Tian, C., Wang, L. & Novick, K. A. Water vapor $\delta^2\text{H}$, $\delta^{18}\text{O}$ and $\delta^{17}\text{O}$ measurements using an off-axis integrated cavity output spectrometer-sensitivity to water vapor concentration, delta value and averaging-time. *Rapid Commun. Mass Spectrom.* **30**, 2077–2086 (2016).
54. Steig, E. *et al.* Calibrated high-precision ^{17}O -excess measurements using cavity ring-down spectroscopy with laser-current-tuned cavity resonance. *Atmos. Meas. Tech.* **7**, 2421–2435 (2014).
55. Schoenemann, S. W., Schauer, A. J. & Steig, E. J. Measurement of SLAP2 and GISP $\delta^{17}\text{O}$ and proposed VSMOW-SLAP normalization for $\delta^{17}\text{O}$ and ^{17}O -excess. *Rapid Commun. Mass Spectrom.* **27**, 582–590 (2013).
56. IAEA: Reference Sheet for VSMOW2 and SLAP2 international measurement standards. *International Atomic Energy Agency (IAEA)* (2009).
57. Angert, A., Cappa, C. D. & DePaolo, D. J. Kinetic ^{17}O effects in the hydrologic cycle: Indirect evidence and implications. *Geochim. Cosmochim. Acta* **68**, 3487–3495 (2004).
58. Luz, B. & Barkan, E. Variations of $^{17}\text{O}/^{16}\text{O}$ and $^{18}\text{O}/^{16}\text{O}$ in meteoric waters. *Geochim. Cosmochim. Acta* **74**, 6276–6286 (2010).
59. Tian, C. *et al.* Stable isotope composition of dew measured from 2014 to 2018 in Namibia, France, and the United States. *PANGAEA* <https://doi.org/10.1594/PANGAEA.934127> (2021).
60. Berman, E. S., Levin, N. E., Landais, A., Li, S. & Owano, T. Measurement of $\delta^{18}\text{O}$, $\delta^{17}\text{O}$ and ^{17}O -excess in water by Off-Axis Integrated Cavity Output Spectroscopy and Isotope Ratio Mass Spectrometry. *Anal. Chem.* **85**, 10392–10398 (2013).
61. Affolter, S., Häuselmann, A. D., Fleitmann, D., Häuselmann, P. & Leuenberger, M. Triple isotope (δD , $\delta^{17}\text{O}$, $\delta^{18}\text{O}$) study on precipitation, drip water and speleothem fluid inclusions for a Western Central European cave (NW Switzerland). *Quat. Sci. Rev.* **127**, 73–89 (2015).
62. Pang, H. *et al.* Spatial distribution of ^{17}O -excess in surface snow along a traverse from Zhongshan station to Dome A, East Antarctica. *Earth Planet. Sci. Lett.* **414**, 126–133 (2015).

Acknowledgements

Funding for this work was made available from the Indiana University-Purdue University Indianapolis Research Support Funds Grant, U.S. National Science Foundation (EAR-1554894), and the National Science Foundation of China (42007155).

Author contributions

C.T. analyzed the samples and wrote the manuscript. K.D. drew the figures and commented on the manuscript. L.W. conceived the idea, collected the samples and edited the manuscript. X.Z., F.L., and W.J. commented on the manuscript. D.B., K.K., and M.M. collected the samples.

Competing interests

The authors declare no competing interests.

Additional information

Supplementary information The online version contains supplementary material available at <https://doi.org/10.1038/s41597-022-01151-6>.

Correspondence and requests for materials should be addressed to L.W.

Reprints and permissions information is available at www.nature.com/reprints.

Publisher's note Springer Nature remains neutral with regard to jurisdictional claims in published maps and institutional affiliations.



Open Access This article is licensed under a Creative Commons Attribution 4.0 International License, which permits use, sharing, adaptation, distribution and reproduction in any medium or format, as long as you give appropriate credit to the original author(s) and the source, provide a link to the Creative Commons license, and indicate if changes were made. The images or other third party material in this article are included in the article's Creative Commons license, unless indicated otherwise in a credit line to the material. If material is not included in the article's Creative Commons license and your intended use is not permitted by statutory regulation or exceeds the permitted use, you will need to obtain permission directly from the copyright holder. To view a copy of this license, visit <http://creativecommons.org/licenses/by/4.0/>.

The Creative Commons Public Domain Dedication waiver <http://creativecommons.org/publicdomain/zero/1.0/> applies to the metadata files associated with this article.

© The Author(s) 2022